CONFORMATIONS OF INSOLUBLE BLOCKS IN SWOLLEN MICELLAR CORES OF MULTIMOLECULAR BLOCK COPOLYMER MICELLES STUDIED BY MONTE CARLO SIMULATION TECHNIQUE

Karel PROCHAZKA and Zuzana LIMPOUCHOVA

Department of Physical and Macromolecular Chemistry, Charles University, 128 40 Prague 2, The Czech Republic

Received November 8, 1993
Accepted January 4, 1994

Monte Carlo simulations of chain conformations in restricted spherical volumes with an increasing radius were performed on a tetrahedral lattice (ca 2 700 to 9 200 lattice sites) at relatively high densities of the occupied lattice sites. A simultaneous self-avoiding walk together with the equilibration algorithm similar to that of Siepmann and Frenkel were used to create the equilibrated multi-chain conformations. (a) A series of simulations was carried out for a constant average segment density, $\langle g_S \rangle = 0.52$, together with the three values of the radius of the sphere, $R = 10\ l$, $12.5\ l$ and $15\ l$ (l is the lattice distance), and various numbers of chains, $N \in \langle 15, 86 \rangle$, and chain lengths, $L \in \langle 31, 163 \rangle$. The results give information on the system behavior and on the effects of: (i) multi-chain conformational correlations, which depend both on N and L, (ii) the L-dependent chain flexibility, and (iii) R-dependent external geometrical constraints. Another two series of data: (b) for a constant average segment density, $\langle g_S \rangle = 0.36$, a constant $N = 21$, and L proportional to R^3, and (c) for $\langle g_S \rangle = 0.36$, $L = 47$ and N proportional to R^3, are shown to give a supplementary detailed information on conformational behavior of individual chains. Various physical quantities (e.g. the densities of chain free ends, $g_F(r)$, or distributions of the tethered end-to-the free end distances, $\rho_{TF}(r_{TF})$, etc.) were calculated in the course of computer simulations and their shapes and physical significance is discussed with respect to the changing values of N, L and R.

Formation of block copolymer micelles from copolymer AB, or ABA in selective solvents (i.e. solvent for one type of blocks, A, and a non-solvent for the other type of blocks, B) is an interesting phenomenon, which plays an important role both in macromolecular and colloid chemistry. Structure and properties of polymeric micelles are controlled by a complex and intricate enthalpy-to-entropy balance in a multicomponent system[1,2].

In the last two decades, a considerable effort has been devoted to develop a successful thermodynamic theory which would explain and possibly also predict details of the behavior of micellar systems in a sufficiently broad region of temperatures, solvent and copolymer concentrations, copolymer compositions and their molar masses. Several theoretical approaches have been recently published[3 – 10]. They are able to explain general principles of micellization equilibria. However, a full quantitative agreement

with reliable experimental data on well-characterized and sufficiently monodisperse micellizing copolymer systems has never been achieved in a broad range of experimental conditions due to various approximate assumptions that had to be adopted by those theories.

Great achievements in computer technology in recent years enabled fairly realistic numerical simulations of a broad spectrum of physical and chemical phenomena. Reliable Monte Carlo simulations of polymeric systems are at present quite common[11 – 15]. Computer simulations of block copolymer micellization processes are however quite rare due to the enormous complexity of the problem and to extremely high demands on computer memory and speed.

Mattice et al. in their seminal works[16 – 18] were able to simulate a spontaneous formation of multimolecular micelles without any limiting assumptions on the behavior of the system. They studied diblock (10A/10B segments) and triblock (5A/10B/5A segments) copolymers in a selective solvent for A blocks. Papers by Mattice et al. are to our knowledge the most rigorous and successful theoretical studies of block copolymer micellization published so far. The authors did not study any details concerning soluble or insoluble block arrangements as their chains were too short for that type of investigation.

In our previous paper[19], we have started a systematic Monte Carlo study of insoluble block conformations in micellar cores. We study conformations of tethered chains in small volumes at high densities. Results of numerical simulations provide information which may be used for thermodynamic description of micellizing systems and for interpretation of physical processes proceeding in micellar cores (such as excitation energy migration[20 – 23], etc.).

In the first paper[19], we have presented a selected part of results of simulations of tethered chain conformations in a spherical cavity containing 2 718 lattice sites on a tetrahedral lattice. The access to a more powerful computer DEC 5000/200 enabled us: (i) to perform computations for systems which we could not study earlier (i.e. for certain combinations of chain numbers, N, and chain lengths, L, for which a high percentage of excluded conformations lead to extremely high computational times on PC 486 – typically several weeks), and (ii) to increase the volume of the spherical cavity up to 300% and to study the influence of the core radius, R, on chain conformations.

Having described the details of simulation technique and the physical meaning of calculated functions earlier[19], we can go deeper into details in the discussion of the thermodynamic behavior of the system.

METHOD

Principles of the simulation technique have been described in details in our previous paper[19]: (i) Conformations of N tethered chains (each containing L segments) in a restricted spherical volume are generated by a simultaneous self-avoiding walk on a te-

trahedral lattice (with a distance l of the lattice sites). All chains start in a narrow spherical surface layer. "Thermal equilibration" of the system, which is necessary to remove a bias of the steadily increasing density of occupied lattice sites during the simultaneous growth of many chains and to circumvent the "attrition problem"[24], proceeds in two steps: (ii) A randomly chosen chain is disregarded and a new chain is grown again in the dense system from a random surface site. This step is repeated ($N^2/2$) times. (iii) To reach the equilibrium of the system, the step (ii) is repeated again ($N^2/2$) times and the Rosenbluth weights[25], $w_i^{(k)}$ in each step i, and weights of resulting chain conformations k, $W_k = \prod_{i=1}^{L} w_i^{(k)}$, are evaluated, ($w_1^{(k)} = 1$, $k = 1, 2$, for an old, or a new conformation, respectively). The new conformation of the chain is accepted according to the modified Metropolis criterion[26] for the factor (W_{new}/W_{old}). A system consisting of the last N accepted chains is considered as one statistically uncorrelated multi-chain conformation which mimics well a randomly chosen micellar core in the thermal equilibrium of the studied micellar system.

The simulation procedure is a specific modification of the algorithm proposed by Siepmann ad Frenkel[15] for dense polymer systems. It is a suitable simulation technique for systems of tethered chains. We have tested also the tree-bonds "crankshaft" motion (a modification of the Verdier algorithm[27]) in the studied system, but the latter was relatively slowly convergent and thus much less efficient than the previous one.

In this paper we consider only the geometrical excluded volume effect of segments. An additional effect of interaction parameters and the *trans*/*gauche* rotational potentials is a subject of an ongoing study and the results will be presented in the next communication.

The presented distributions were in most cases calculated on the basis of 10^4 statistically uncorrelated multi-chains arrangements ($5 \cdot 10^3$ arrangements were used for $R = 15\ l$, since those simulations took typically several days on DEC 5000/200). A simulation of each multi-chain arrangement starts by a totally independent simultaneous self-avoiding walk and continues by the above described equilibration, which represents a generation of N^2 new chain arrangements (generally 10^4 to 10^5 segment positions). It means that the data are are based on 10^8 to 10^9 successfully generated segment positions.

Physical nature of the problem does not require to use the periodic boundary conditions.

Calculations were performed on a DEC 5000/200 computer. An original program was written in FORTRAN 77. The longest calculations took up to two weeks of the CPU.

RESULTS AND DISCUSSION

In our previous calculations[19] we have shown that the actual segment density, $g_S(r)$, asa function of the distance from the sphere center, r, is almost constant for higher densities of the occupied lattice sites, $\langle g_S \rangle > 0.36$, and for longer chains (depending on $\langle g_S \rangle$

and N; typically $L > 40$, for $\langle g_S \rangle = 0.36$) and does not nearly depend on the surface density of the tethered chain ends, $\langle g_{int} \rangle$. This holds generally within the whole sphere, except the part in a narrow surface region. Such a situation is typical for spherical cores of multimolecular copolymer micelles in selective solvents. It is an experimentally established fact that micellar cores are uniform[1,28] and the segment density inside the core is constant (only in the core/shell interfacial region, the insoluble and soluble blocks are partially intermixed). In this paper we present results that model real cores of polymeric micelles in solutions.

The aim of this paper is to study the influence of geometrical restrictions on conformations and orientations of individual tethered chains and their parts. Conformations of chains in micellar cores depend on the number of chains, N, chain lengths (i.e. the number of segments, L) and the number of all lattice sites N_{tot} in the sphere (i.e. the volume of the sphere, $V_{sp} = (4/3)\,\pi\,R^3$). In the preceding paper[19] we have shown that the average segment density, $\langle g_s \rangle = (N\,L/N_{tot})$, predetermines to a certain degree the behavior of the system. Nevertheless, this factor alone – even though very important – does not control all properties of the system. Results for constant values of the average segment density, $\langle g_S \rangle$, suggest that the calculated conformational characteristics of chains depend both on N and L. Unfortunately, values of (N L) had to be kept constant in our previous calculations (in order to get the constant density) and we were unable to study independent effects of varying N and L. In this paper we vary also the sphere radius R (i.e. the number N_{tot}) and we can thus study an indirect effect of the chain length, L, at constant N and constant $\langle g_S \rangle$. This enables us to investigate the influence of an increased conformational flexibility of longer chains on the structural characteristics of micellar cores.

For the type of simulations, where several parameters (N, L and N_{tot}) are varied, and results depend on the average segment density, $\langle g_S \rangle = (N\,L/N_{tot})$, on the ratio (L/N_{tot}), etc., an interpretation of the results must be done with a high care. A complete presentation of the data for too many combinations of N, L and N_{tot} would exceed the size of a reasonable paper. To offer the most comprehensive outline of the behavior of tethered chains in restricted volumes at high segment densities, we have chosthe following sets of data:

a) First we present a series of selected results for three values of the core radius, $R = 10\,l$, $12.5\,l$ and $15\,l$, and for a constant average segment density, $\langle g_S \rangle = 0.52$. (The precise value of $\langle g_S \rangle$ is 0.515 ± 0.002; small variations in $\langle g_S \rangle$ are caused by the fact that both N and L assume only integer numbers.) The same set of several increasing surface densities of tethered ends, $\langle g_{int} \rangle = (N/N_{int})$, is used for all R values; N_{int} is the number of the lattice sites in a narrow spherical surface layer (in the core/shell interface). Since N_{tot} is proportional to R^3 and N_{int} to R^2, the ratio (L/R) is kept constant in simulations, corresponding to the same surface density. A combined effect of (i) the decreasing chain stiffness with increasing L, and (ii) the decreasing importance of

geometrical constraints with increasing radius of the cavity, R, will be discussed for this series of data.

b) Second, we give data for three increasing values of R and L and for a constant segment density, $\langle g_S \rangle = 0.36$, and a constant number of chains, $N = 21$. In that case, the ratios $(\langle g_S \rangle / N)$ and (L/R^3) are constant and L is therefore proportional to R^3.

c) The last series gives data for increasing R and for constant values $L = 47$ and $\langle g_S \rangle = 0.36$. Here the number of chains, N, increases, since it depends on R^3.

Dependences of calculated structural characteristics of the system on L, for constant $\langle g_S \rangle$ and N, describe reasonably well the influence of varying chain stiffness which decreases with increasing chain length, L, whereas the dependences on R (i.e. on N_{tot}) for constant $\langle g_S \rangle$ and L describe reasonably well the influence of geometrical constraints. We are aware, however, that each of the shown functions describes in full rigor only the behavior of the system under the given combination of parameters used in a particular simulation.

Several distribution functions, which describe conformations of individual chains in micellar cores, may be easy calculated during numerical simulations: (i) distribution of the free-to-tethered chain end distances, $\rho_{TF}(r_{TF})$, (ii) distribution of the distances of the centers of gravity of chains from the tethered ends, $\rho_{TC}(r_{TC})$, (iii) distribution of the free end-to-the center of gravity distances, $\rho_{FC}(r_{FC})$ and (iv) distribution of radii of gyration of individual chains, $\rho_R(R_g)$. Three following functions show collective structural characteristics of chains in cores: (v) segment density, $g_S(r)$, as a function of the distance from the core center, r, – not shown in this paper, (vi) density of the free ends, $g_F(r)$, and (vii) density of the gravity centers, $g_C(r)$. Orientations of individual chains in an equilibrium micellar core may be further described by angular distributions of various structural characteristics (e.g. directions of the end-to-end vectors etc., with respect to the radial orientation), and by projections of various distance-vectors into the radial direction, or into the direction of the first-to the second segment connection. The angular distributions and the distributions of various projections into the selected directions are subjects of the next paper of this series[29].

Distribution of the End-to-End Distances and the Related Functions

Figures 1*a* – 1*c* show distributions of the tethered-to-free chain end distances, $\rho_{TF}(\rho_{TF})$, for three spherical micellar cores with increasing radius, $R = 10\ l$, $12.5\ l$ and $15\ l$. Four curves describing behavior of various multi-chain systems (differing in N) are shown for each R-value. A constant average segment density $\langle g_S \rangle = 0.52$ is kept for all 12 curves. In order to keep a constant value of $\langle g_S \rangle$, an increase in the number of chains, N, (in each series of curves for a particular R) is accompanied by a concomitant decrease in the chain length, L. Each triplet of curves, i.e. curves *1* in Figs 1*a* – 1*c*, curves *2*, *3* and *4* in all three figures, correspond to the same surface density; $\langle g_{int} \rangle = 0.45$ (*1*), 0.35 (*2*), 0.25 (*3*) and 0.15 (*4*).

Two more figures (Figs 1*d* and 1*e*), each showing three selected curves for a constant average segment density, $\langle g_S \rangle = 0.36$, and an increasing core radius, *R*, are supplemented to deepen the insight into the conformational behavior of chains in micellar cores. In Fig. 1*d*, the number of chains, *N*, is constant and the chain length, *L*, increases together with *R* to secure a constant value of $\langle g_S \rangle$. In Fig. 1*e*, the chain length, *L*, is constant and the number of chains varies to keep a constant $\langle g_S \rangle$ for increasing values of *R*.

A complex conformational behavior which is caused by: (i) the increasing chain flexibility with increasing chain length, *L*, and (ii) the slightly decreasing importance of external geometrical constraints with increasing core radius, *R*, is clearly evident from a comparison of individual curves in Figs 1*a* – 1*e*. For a detailed discussion of their shapes, it is necessary to realize that the magnitude of $\rho_{TF}(\rho_{TF})$ does neither directly depend on *N*, nor on *L* – the function $\rho_{TF}(r_{TF})$ is a normalized end-to-end distribution for one chain. Its magnitude depends however on the term $(N_{tot})^{-1}$, since the values for given distances r_{TF} are normalized by numbers of all lattice sites in narrow partial spherical layers of the radius r_{TF} and the thickness $\Delta = 1.25\ l$ – see Fig. 2 and also the details of the calculation procedure in ref.[19].

The following findings are of interest:

a) The shape of the $\rho_{TF}(r_{TF})$ curves is essentially the same for all studied systems, regardless of particular values of *N* and *L*. The curves show quite pronounced maxima between $r_{TF} = 5\ l$ and $7.5\ l$. They differ considerably from distributions for free flexible chains with a negligible excluded volume effect and remind those for self-avoiding isolated chains. The shape of $\rho_{TF}(r_{TF})$ curves in the studied system with maxima positions which depend only very little on *L*, is an understandable result of a combined effect of external geometrical constraints (a small spherical volume of the core) together with a relatively high chain rigidity (short chains on a tetrahedral lattice, i.e. on a lattice with a low coordination number, behave as quite stiff chains) and the excluded volume effect.

b) In a given core (with a constant radius, *R*), maxima are more pronounced for shorter chains due to the already mentioned restricted flexibility of shorter chains.

c) The longer are the chains, the more important are the fractions of "stretched" chains with $r_{TF} \rightarrow 2\ R$. This effect is very clearly evident for $R = 10\ l$ and $L = 93$. In that case, the limiting value of $\rho_{TF}(r_{TF} \rightarrow 2\ R)$ represents ca 30% of the maximum value of $\rho_{TF}(r_{TF})$. This behavior, which is a relatively straightforward consequence of external geometrical constraints, precludes a general existence of an "excluded zone" close to the core surface, where the free ends could not be located (see the further discussion to Fig. 4 – the density of the free ends as a function of the distance from the core center, $g_F(r)$). Such an "excluded zone" was theoretically predicted for systems of chains tethered to a convex surface (located outside the sphere) by Semenov et al.[30] on

the basis of a self-consistent field theory, but it was not confirmed by the subsequent Monte Carlo simulations for those systems[31].

d) With the increasing *R*-values, all curves become broader and flatter due in a major part to an increased flexibility of longer chains which had to be used in systems with higher radii, *R*, in order to get a constant segment density, $\langle g_S \rangle$, for all systems, and to a minor part to less important geometrical constraints.

More information on the conformational behavior of the multi-chain system in a limited spherical volume may be gained from a comparison of curves in Figs 1*a* – 1*c* with those in Fig. 1*d* and 1*e*.

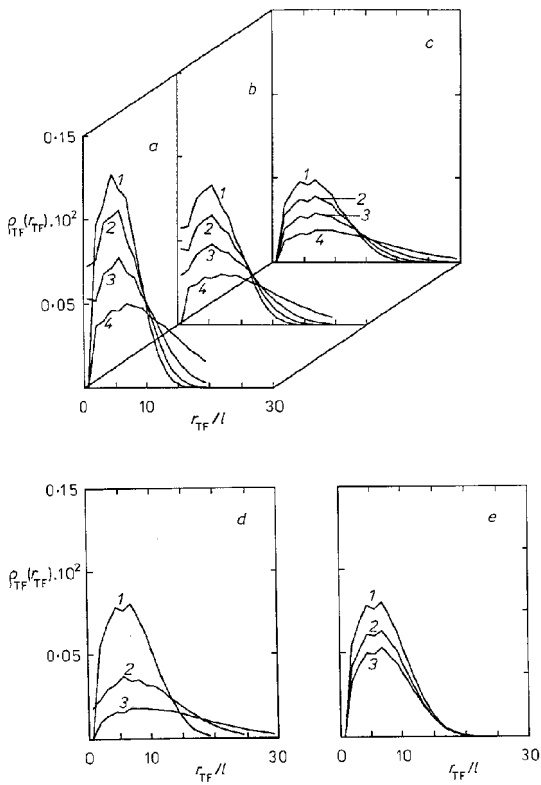

FIG. 1

Distribution function of the tethered-to-free end distances of individual chains in spherical micellar cores, $\rho_{TF}(r_{TF})$, for two constant segment densities: $\langle g_S \rangle$ = 0.52 (*a*, *b*, *c*) and $\langle g \rangle_S$ = 0.36 (*d*, *e*). Values of the other parameters: *a* *R* = 10 *l*, *N*/*L* = 45/31 (*1*), 35/40 (*2*), 25/56 (*3*) and 15/93 (*4*); *b* *R* = 12.5 *l*, *N*/*L* = 68/40 (*1*), 53/52 (*2*), 38/72 (*3*) and 23/119 (*4*); *c* *R* = 15 *l*, *N*/*L* = 86/55 (*1*), 67/71 (*2*), 48/99 (*3*) and 29/163 (*4*); *d* constant number of chains, *N* = 21 and *L* = 47, *R* = 10 *l* (*1*), *L* = 92, *R* = 12.5 *l* (*2*) and *L* = 159, *R* = 15 *l* (*3*); *e* constant chain length, *L* = 47 and *N* = 21, *R* = 10 *l* (*1*), *N* = 41, *R* = 12.5 (*2*) and *N* = 71, *R* = 15 *l* (*3*)

Figure 1*d* shows a marked effect of the increasing chain flexibility with increasing L on the multi-chain arrangements which leads to quite flat distributions for high L (e.g. an almost uniform distribution for $L = 159$ and $R = 15\ l$ – curve *3* in Fig. 1*d*. The ratio of (L/R^3) is kept constant for all curves which minimizes an effect of changing geometrical constraints with increasing R. Curves for a constant $L = 47$ and increasing R and N are shown in Fig. 1*e*. A comparison of individual curves is slightly surprising. Their shapes (including positions of maxima) are essentially the same for all three R-values. Differences in magnitudes of individual curves are caused mainly by the R-dependant normalization factors (see Fig. 2). The obtained results suggest that the end-to-end distributions depend mainly on the chain length, L, and do not nearly depend on R. It may be concluded that the influence of the external geometrical restrictions, even though very important (it predetermines the general shape of the distribution functions), does not change fast with increasing R in the region of the studied volumes. Similar conclusions may be drawn from the results concerning the distributions of the radii of gyration, R_g, (see later).

We would like to emphasize that the presented distributions are angular averages of the calculated functions for all allowed orientations of the end-to-end distances with respect to the radial direction. Functions $P_{TF}(r_{TF}, \vartheta)$ which describe correlated distributions of the end-to-end distances and their angular orientations under various conditions, are a subject of the ongoing studies[32].

Figure 3 shows the number fractions of chains with particular end-to-end separations in equilibrium cores, $n_{TF}(r_{TF})$, for the same systems as in Figs 1*a* – 1*c*. Distributions $\rho_{TF}(r_{TF})$ and $n_{TF}(r_{TF})$ may be readily recalculated from each other. The latter distribution is presented because it gives a better idea of the number-fractions of chains with given r_{TF} distances.

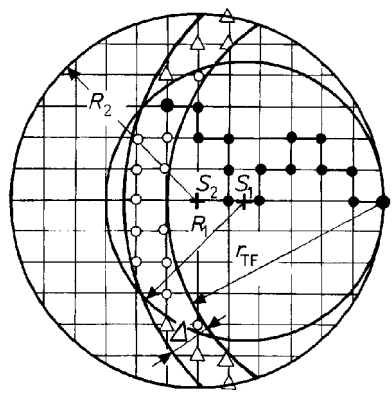

FIG. 2
A schematic two-dimensional representation of the evaluation of the R-dependent normalization factor in functions $\rho_{TF}(r_{TF})$, etc.

Density of the free-chain-ends within the micellar core is shown in Fig. 4 for the same systems as in Fig. 1 (all figures with the same structure as Fig. 1 show distribution functions for the same systems as in Fig. 1). All curves show an evident increase towards the core center. This increase is more pronounced in systems with high numbers of relatively short chains (i.e. in systems with an elevated surface density of tethered chains, $<g_{int}>$) and in systems with small core radii, R. The fraction of the free ends located close to the surface differs in all cases significantly from zero. In order to get the number of the free ends, $n_F(r)$, in the distance r from the center, the $g_F(r)$ value must be multiplied by the number of the lattice sites in a spherical layer with the radius r and the thickness $\Delta = 1.25\ l$. The numbers $n_F(r)$ are proportional to r^2 which means that the number of the free ends close to the surface is quite important in the studied system. This result together with the already discussed shape of $\rho_{TF}(r_{TF})$ preclude a general existence of the "excluded zone" (cf. discussion concerning Fig. 1). A forma-

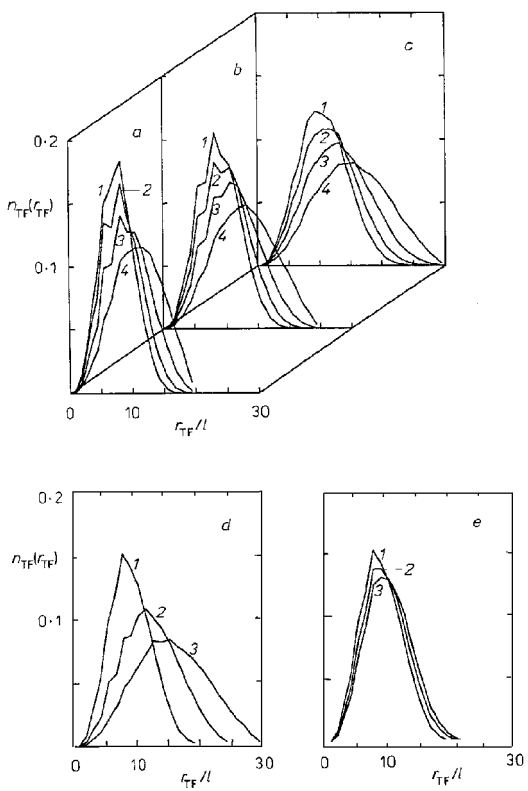

FIG. 3
Number fractions, $n_{TF}(r_{TF})$, of chains with given end-to-end distances corresponding to distribution functions in Figs 1*a* – 1*e*

tion of the "excluded zone" does not seem probable in closed concave systems. Its existence in systems of polymers grafted to the convex surfaces is rationalized by the fact that the segment density decreases spontaneously in the perpendicular direction from the surface and the natural tendency of the system is to minimize its free energy by a partial stretching of polymer chains and placing them into a less concentrated region. A similar condition is not met in closed systems.

Figure 4e shows density of the free ends, $g_F(r)$, for a constant chain length, L, and increasing values of N and R. All calculated curves rise with the decreasing distance from the center, r. Their slopes do not depend on R, however quite a considerable fraction of chains reaches into the central part of the core in all three cases. Since $\rho_{TF}(r_{TF})$ does not nearly depend on R, this effect is probably caused by slightly different angular arrangements of chains in those three systems.

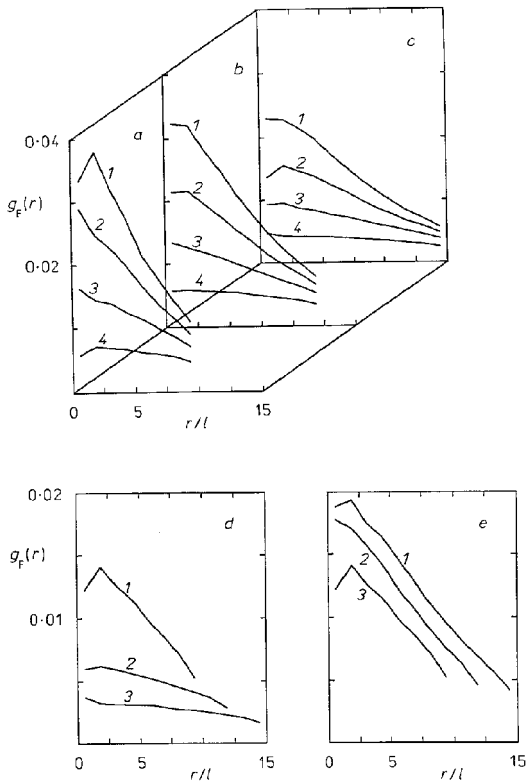

FIG. 4
Density of the free chain ends within a core as a function of the distance from the core center, $g_F(r)$, for the same systems as in Fig. 1

Distribution of the End-to-Gravity Center Distributions

Three further figures (Figs 5 – 7) show density of the centers of gravity of individual chains in micellar cores, $g_C(r)$, and distributions of the distances of gravity centers from either the tethered, or the free chain ends, $\rho_{TC}(r_{TC})$ and $\rho_{FC}(r_{FC})$, respectively.

Density of gravity centers, $g_C(r)$, for systems with short chains is negligible in the central region (i.e. for $r \to 0$) and rises quite fast with the increasing r. A clearly pronounced and sharp maximum is reached fairly close to the surface – in the distance ca 3 l from the surface. This position is almost independent of R. Then $g_C(r)$ drops steeply to zero for $r \to R$. The initial rise is less steep for larger R, but the final drop does not nearly depend on R. With the increasing chain length, the curves become flatter and broader and maxima are shifted to lower r values and the density in the central region is quite high.

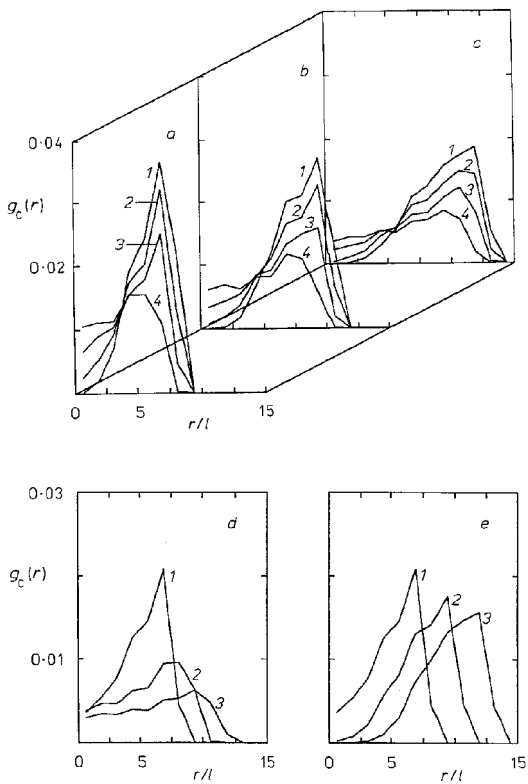

FIG. 5
Density of the gravity centers of individual chains in a spherical core, $g_C(r)$, for the same systems as in Fig. 1

Interesting shapes show distributions of the tethered end-to-the center of gravity distances, $\rho_{TC}(r_{TC})$, and the free end-to-the center of gravity distances, $\rho_{FC}(r_{FC})$, (Figs 6 and 7). All obtained curves, $\rho_{TC}(r_{TC})$, are zero for $r_{TC} \to 0$, then they rise steeply and reach sharp maxima at r_{TC} ca $4 - 5\ l$ and drop again quite fast to zero. Curves are broader and asymmetrical (with respect to the maxima positions) for longer chains, their maxima are shifted to higher r_{TC} and their tails reach into the region of $r_{TC} > R$. Distributions $\rho_{TC}(r_{TC})$ in Fig. 6*e* exhibit a similar behavior as $\rho_{TF}(r_{TF})$ in Fig. 1*e*: Individual curves for a constant $<g_S>$) and L do not almost depend on R.

Distributions of the free end-to-the gravity center distances, $\rho_{FC}(r_{FC})$, are qualitatively similar to those for free flexible chains with maxima at $r_{FC} \to 0$. Changes in N, L and R seem to have a similar effect on the widths of both distributions and on the heights of their maxima.

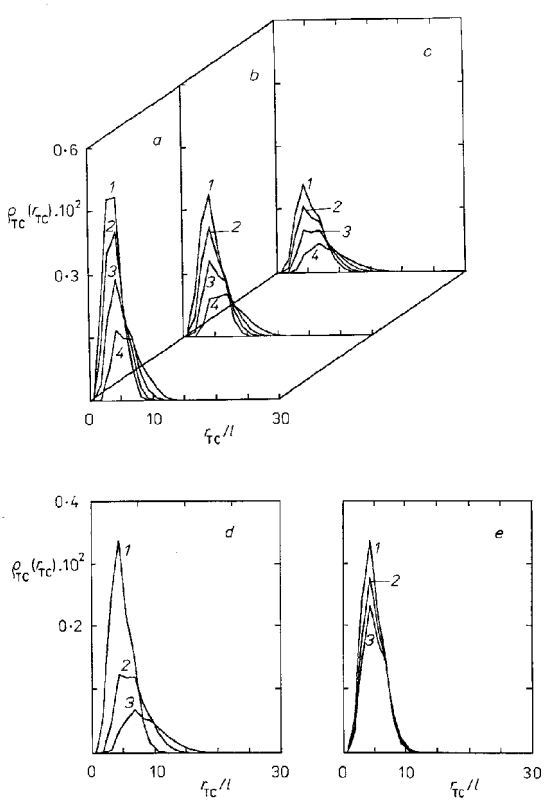

FIG. 6
Distribution function of the tethered end-to-the gravity center distances, $\rho_{TC}(r_{TC})$, for the same systems as in Fig. 1

A comparison of both types of curves suggests that the "tethered halves" of chains are partially oriented and stretched into the radial direction in the vicinity of the concave surface and behave as quite "stiff" chains as compared with the "free halves" which are more coiled and oriented fairly random into all possible directions (a considerable fraction of chains may turn back towards the tethered end).

Very interesting conclusions may be drawn from a comparison of the maxima positions in $g_C(r)$ and $\rho_{TC}(r_{TC})$. The highest density of the gravity centers, $g_C(r)$, is in the distance ca 3 l from the core surface (in all systems), whereas the maximum positions of $\rho_{TC}(r_{TC})$ are attained for $r_{TC} = 5\ l$. This means that despite the preferential radial orientation of chains (mainly of their "tethered halves") a fairly considerable fraction of chains decline appreciably from the radial direction. This finding was also confirmed by calculations of the angular distributions – see next part of this series[29].

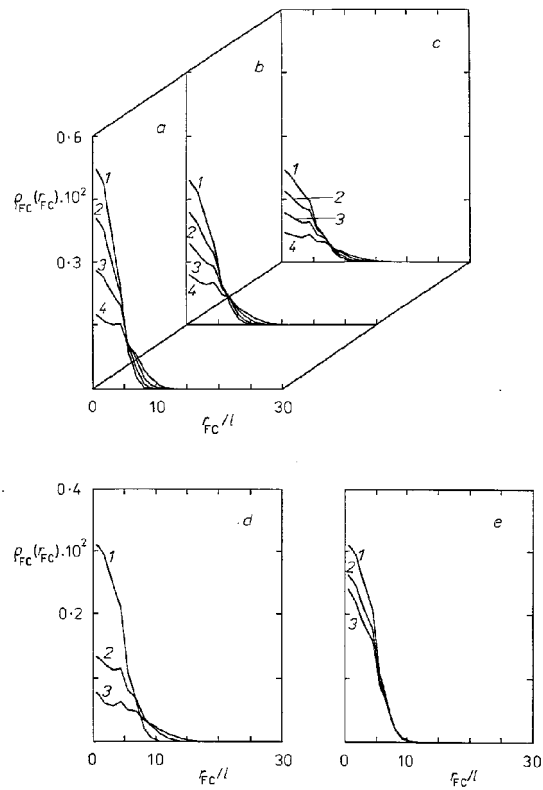

FIG. 7
Distribution function of the free end-to-the gravity center distances, $\rho_{FC}(r_{FC})$, for the same systems as in Fig. 1

Other Conformational Characteristics

Distribution of the free-end-pair-distances of different chains, $\rho_{FF}(r_{FF})$, and corresponding number fractions of pairs with particular r_{FF} values, $n_{FF}(r_{FF})$, are shown in Figs 8 and 9. These functions are very important for interpretation of experimental time-resolved fluorescence anisotropy decays in micellar systems with the end-tagged copolymers[33,34]. Values of $\rho_{FF}(r_{FF})$ for given r_{FF} are normalized by numbers of all possible pairs of the lattice sites separated by $(r_{FF} \pm \Delta)$ – see previous paper[19], and therefore a constant function $\rho_{FF}(r_{FF})$ represents a fully random distribution of the free ends of different chains.

Fairly random distributions of the free-end-pairs, $\rho_{FF}(r_{FF})$, were obtained in systems with a large $R = 15\ l$. The degree of the random character of that distribution in a broad range of r_{FF} is controlled mainly by the external constraints and it is therefore very

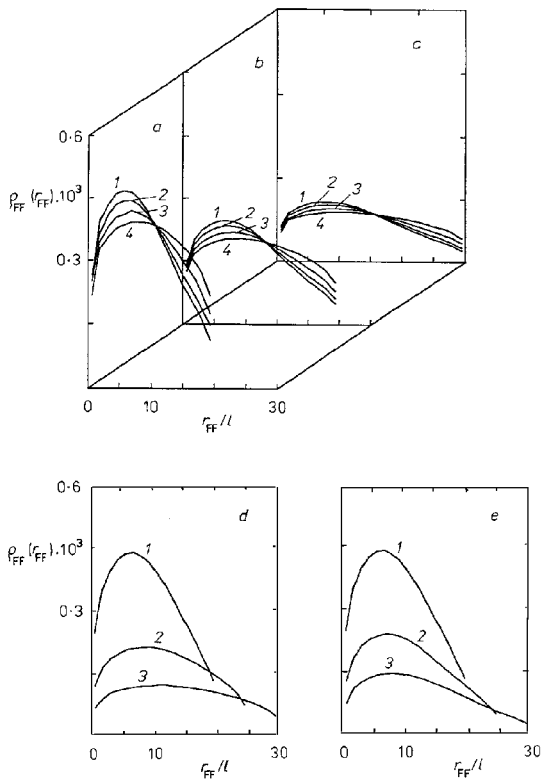

FIG. 8
The pair distribution function of the free-end-distances of different chains, $\rho_{FF}(r_{FF})$, for the same systems as in Fig. 1

sensitive to changing R (all the other calculated functions are more sensitive to changes in $\langle g_S \rangle$, N and L than in R).

Figure 10 shows distributions of the radii of gyration of individual chains, $\rho_R(R_g)$. These distributions are quite narrow with maxima at relatively low values of R_g (as compared with those of free flexible chains) and are almost symmetrical with respect to the maxima positions. They depend mainly on L and are insensitive to small changes in R – see Fig. 10*e*.

Scaling Properties

The average values of various conformational characteristics of individual chains (based on the distributions presented above) are given in Tables I, II and III for cores with R = 10 l, 12.5 l and 15 l, respectively. They give a compressed and comprehensive

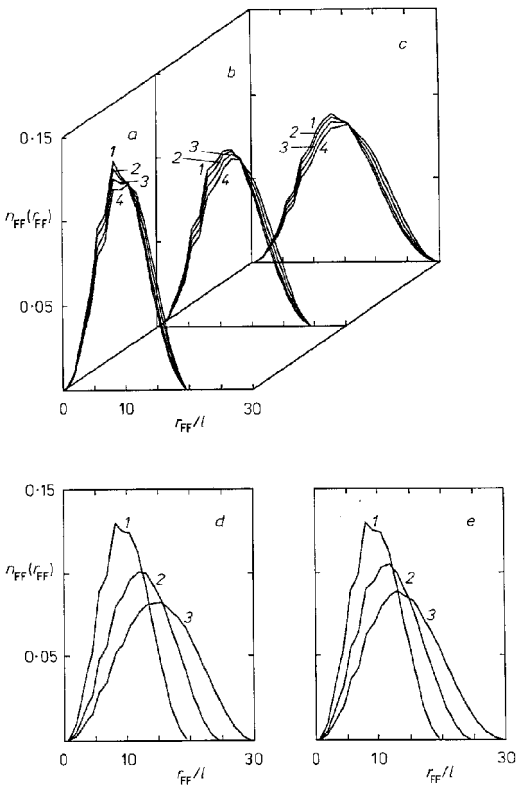

FIG. 9
The number fraction of the free-end-pairs with given distances, $n_{FF}(r_{FF})$, for the same systems as in Figs 8*a* – 8*e*

quantitative characterization of the studied systems. Since the average values were calculated from the already discussed distributions, the qualitative trends agree with the previous conclusions and will not be repeated. Nevertheless, dependences of various root-mean-square average distances on the chain length, L, give quite important supplementary information on the system behavior. The selected ln (R_g/l) and ln ($\langle r_{TF}^2\rangle^{1/2}/l$ vs ln L plots are shown in Fig. 11. They are almost linear in the region of L which was accessible for our simulations (they are slightly curved for the lowest L).

Scaling parameters, a, do not nearly depend on R, but they are different for ln (R_g/l), $a = 0.41 \pm 0.01$, and ln ($\langle r_{TC}^2\rangle^{1/2}/l$), $a = 0.33 \pm 0.01$ and are very low in comparison with the value for the self-avoiding random walk. The scaling parameter for the root-mean-square average end-to-end distance for long isolated chains is $a = 0.588$ (refs[11,35,36]) for a three-dimensional self-avoiding walk at any type of the lattice (for an

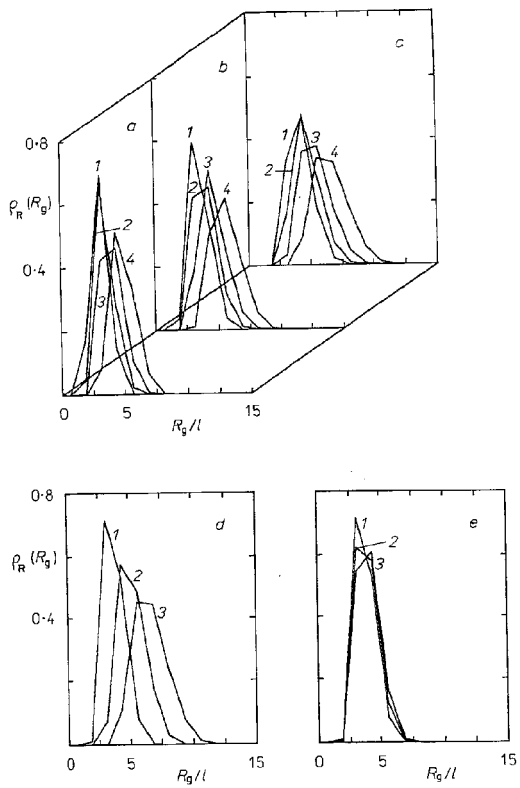

FIG. 10
Distribution of the radii of gyration of chains in spherical cores, $\rho_R(R_g)$, for the same systems as in Fig. 1

TABLE I

Values of the root-mean-square averages and averages of the absolute values of: end-to-end distances, $\langle (r_{TF})^2 \rangle^{1/2}$, tethered/or free end-to-gravity center distances, $\langle (r_{TC})^2 \rangle^{1/2}$, $\langle (r_{FC})^2 \rangle^{1/2}$, respectively, and values of the radius of gyration. R_g for systems studied in the core with the radius $R = 10\ l$, (10^5 cores); N is the number of the tethered chains and L is the number of their segments

	$\langle g_S \rangle = 0.5$				$\langle g_S \rangle = 0.36$
N/L	15/93	25/56	35/40	45/31	21/47
$\sqrt{\langle r^2_{TF} \rangle}$	11.61	10.15	8.96	8.15	9.71
$\sqrt{\langle r^2_{TC} \rangle}$	7.57	6.31	5.44	4.89	5.94
$\sqrt{\langle r^2_{FC} \rangle}$	6.34	5.43	4.76	4.28	5.17
R_g	4.86	4.00	3.45	3.09	3.76
$\langle \lvert r_{TF} \rvert \rangle$	10.97	9.55	8.44	7.70	9.16
$\langle \lvert r_{TC} \rvert \rangle$	7.27	6.05	5.22	4.71	5.71
$\langle \lvert r_{FC} \rvert \rangle$	5.94	5.07	4.46	4.02	4.84

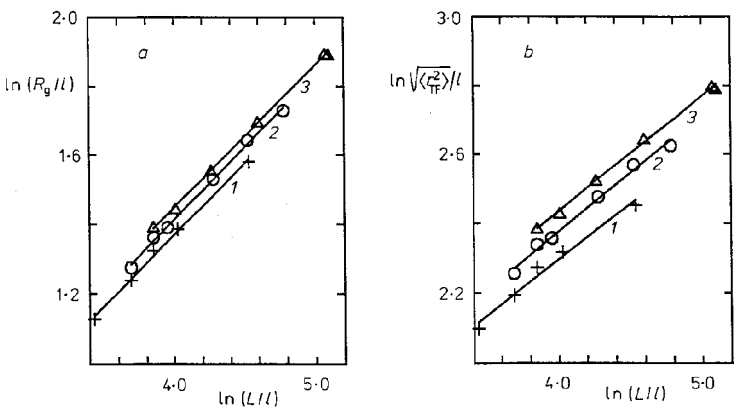

FIG. 11

The ln–ln plot *a* of the radii of gyration of individual chains, R_g, and *b* of the end-to-end root-mean-square distances, $\langle (r_{TF})^2 \rangle^{1/2}$, versus the chain length, L, for a constant $\langle g_S \rangle = 0.52$ and $R = 10\ l$ (*1*), $R = 12.5\ l$ (*2*), and $R = 15\ l$ (*3*)

TABLE II

The same average values as in Table I for systems studied in the core with the radius $R = 12.5\ l$, (10^5 cores)

	$\langle g_S \rangle = 0.5$				$\langle g_S \rangle = 0.36$	
N/L	23/119	38/72	53/52	68/40	21/92	41/47
$\sqrt{\langle r^2_{TF} \rangle}$	13.80	11.89	10.57	9.55	13.05	10.36
$\sqrt{\langle r^2_{TC} \rangle}$	8.87	7.34	6.42	5.73	8.18	6.25
$\sqrt{\langle r^2_{FC} \rangle}$	7.48	6.35	5.58	5.00	7.00	5.45
R_g	5.63	4.62	4.02	3.58	5.17	3.90
$\langle \lvert r_{TF} \rvert \rangle$	13.00	11.16	9.93	9.00	12.28	9.77
$\langle \lvert r_{TC} \rvert \rangle$	8.49	7.02	6.15	5.51	7.84	6.01
$\langle \lvert r_{FC} \rvert \rangle$	6.98	5.92	5.21	4.68	6.54	5.10

TABLE III

The same average values as in Table I for systems studied in the core with the radius $R = 15\ l$, ($5 \cdot 10^4$ cores)

	$\langle g_S \rangle = 0.5$				$\langle g_S \rangle = 0.36$	
N/L	29/163	48/99	67/71	86/55	21/159	71/47
$\sqrt{\langle r^2_{TF} \rangle}$	16.32	14.09	12.48	11.36	16.42	10.88
$\sqrt{\langle r^2_{TC} \rangle}$	10.48	8.72	7.61	6.85	10.52	6.53
$\sqrt{\langle r^2_{FC} \rangle}$	8.84	7.51	6.59	5.94	8.87	5.64
R_g	6.63	5.45	4.73	4.25	6.65	4.02
$\langle \lvert r_{TF} \rvert \rangle$	15.34	13.20	11.71	10.67	15.47	10.27
$\langle \lvert r_{TC} \rvert \rangle$	10.01	8.33	7.27	6.56	10.07	6.28
$\langle \lvert r_{FC} \rvert \rangle$	8.23	6.98	6.14	5.54	8.27	5.28

intersecting random walk, $a = 0.5$). These results are in a good agreement with the previous conclusions: The conformational behavior of individual chains in relatively small micellar cores at high segment densities is strongly affected by severe geometrical constraints. This is manifested by low values of scaling parameters in various ln–ln plots. The external constraints are important and relax only very little with increasing core radius. This is the reason why values of scaling parameters (and other structural characteristics) do not nearly depend on R.

There is an interesting question concerning changes in the conformational behavior of the studied system in a broad range of segment densities and a comparison of various distributions at relatively high densities with those for one, two, etc. tethered chains in an almost empty spherical volume. Systems with low numbers of chains do not model realistic micellar cores and a detailed comparison will be published elsewhere. Nevertheless we feel that a brief general remark in that respect may help to elucidate the roles of: (i) the primary effect of external geometrical constraints and (ii) an induced inter-chain correlation effect in dense and constrained multi-chain systems.

It is well-known that the conformational characteristics of chains in dense polymer systems are almost identical with those of corresponding isolated chains (i.e. in an infinitely diluted solution) under the ϑ-conditions. A question arises if a similar conformational behavior is conserved also in restricted geometries, i.e. if certain properties of tethered chains in (a) dilute; and (b) dense and constrained systems are similar to each other.

Results of simulations suggest that the conformational behavior of short and rigid chains does not change much with the changing segment density, whereas the conformational characteristics of dense long chain systems differ considerably from the constrained few chain systems.

In all cases, the role of external geometrical constraints is more important than the role of the inter-chain correlations which may be generally expected in dense multi-chain systems.

CONCLUSIONS

a) A significant effect of geometrical constraints on chain conformations is evident from comparisons of all calculated distributions with those for free flexible chains.

b) Results of calculations for various R show that in relatively small cores studied in this paper, the effect of external geometrical constraints on the behavior of the multi-chain system is severe and relaxes only little with the increasing sphere radius R.

c) The data for systems with increasing R (and L proportional to R^3) allow to study the effect of the increasing chain flexibility with increasing chain length, L, in cores with an approximately constant effect of geometrical constraints. This effect is quite significant and almost all calculated distribution functions are more sensitive to change-

s in the chain length, L, than to changes in the number of chains, N, or the sphere radius, R.

d) It may be inferred from the simulated data that the "tethered halves" of chains are preferentially radially oriented and are more "stiff" than the "free halves", which are quite randomly oriented in space with respect to the gravity centers.

e) The ln–ln plots of the end-to-end distances, versus the chain length, L, are slightly curved even in a relatively narrow range of the studied L, and the average scaling parameter, a ca 0.36, is very low as a result of the severe geometrical constraints.

f) Comparisons of various conformational characteristics of individual chains with each other suggest that in spite of the preferential radial orientation of chains in cores, a considerable fraction of chains differ appreciably from the radial direction.

g) Simulated conformational characteristics of individual chains presented in this paper are suitable approximate functions for the thermodynamic description of block copolymer micellar systems. In this paper we do not take into account the thermodynamic interactions which precludes to minimize the Gibbs free energy of the system and to assess the correct values of micellar parameters. However, general properties and shapes of many functions, e.g. $\rho_{TF}(r_{TF})$, etc., depend only little on the actual values of both $<g_S>$ and R (in the region of the studied values). Their knowledge is very helpful for any considerations concerning the thermodynamics of micellar systems.

The authors are very obliged to Prof. P. Munk from the University of Texas at Austin, U.S.A., for helpful discussions and suggestions concerning the thermodynamic aspects of the system behavior. The authors thank also to the Ministry of Education of the Czech Republic for the financial support of this work (Grant No. FDR 0145) and to the grant Agency of the Czech Republic (Grant No. 203/93/2287).

REFERENCES

1. Tuzar Z., Kratochvil P. in: *Surface and Colloid Science* (E. Matijevic, Ed.), Vol. 15, p. 1. Plenum Press, New York 1993.
2. Ellias H.-G., Barrais R.: Chimia *21*, 53 (1967).
3. de Gennes P. G. in: *Solid State Physics* (J. Liebert, Ed.), Suppl. 14, p.1. Academic Press, New York 1978; de Gennes P. G.: *Scaling Concepts in Polymer Physics*. Cornell University, Ithaca 1979.
4. Leibler L., Orland H., Wheeler J. C.: J. Chem. Phys. *79*, 3550 (1983).
5. Whitmore D., Noolandi J.: Macromolecules *18*, 657 (1985).
6. Meier D. J.: J. Polym. Sci., C *26*, 81 (1969).
7. Helfland E., Sapse A. M.: J. Chem. Phys. *62*, 1327 (1975).
8. Nagarajan R., Ganesh K.: J. Chem. Phys. *90*, 5843 (1989).
9. ten Brinke G., Hadziioannou G.: Macromolecules *20*, 486 (1978).
10. Halperin A.: Macromolecules *20*, 2943 (1987).
11. Kremer K., Binder K.: Comp. Phys. Rep. *7*, 259 (1988).
12. Allen M. P., Tildesley D. J.: *Computer Simulations of Liquids*. Clarendon Press, London 1986.
13. Geyler S., Pakula T., Reitter J.: J. Chem. Phys. *92*, 2676 (1990).

14. Reitter J., Edling T., Pakula T.: J. Chem. Phys. *93*, 837 (1993).
15. Siepmann J. I., Frenkel D.: Mol. Phys. *75*, 59 (1992).
16. Rodrigues K., Mattice W. L.: J. Chem. Phys. *94*, 761 (1991).
17. Rodrigues K., Mattice W. L.: Langmuir *8*, 456 (1992).
18. Wang Y., Mattice W. L., Napper D. H.: Macromolecules *25*, 4073 (1992); Wang Y., Mattice W. L., Napper D. H.: Langmuir *9*, 66 (1993).
19. Limpouchova Z., Prochazka K.: Collect. Czech. Chem. Commun. *58*, 2290 (1993).
20. Gochanour C. R., Andersen H. C., Fayer M. D.: J. Chem. Phys. *70*, 4254 (1979).
21. Loring R. F., Andersen H. C., Fayer M. D.: J. Chem. Phys. *76*, 2015 (1982).
22. Frederickson G. H., Andersen H. C., Frank C. W.: J. Phys. Chem. *79*, 3572 (1983).
23. Byers J. D., Parsons W. S., Webber S. E.: Macromolecules *25*, 5935 (1993).
24. Binder K., Heerman D. W.: *Statistical Physics* 80, *Springer Series in Solid State Physics*, p. 10. Springer, Berlin 1988.
25. Rosenbluth M. N., Rosenbluth A. W.: J. Chem. Phys. *23*, 356 (1955).
26. Metropolis N., Rosenbluth A. W., Rosenbluth M. N., Teller A., Teller H.: J. Chem. Phys. *21*, 1087 (1953).
27. Verdier P. H., Stockmayer W. H.: J. Chem. Phys. *36*, 227 (1962).
28. Cheng P.-L., Berney C. V., Cohen R. E.: Macromolecules *21*, 3442 (1988).
29. Limpouchova Z., Prochazka K.: Collect. Czech. Chem. Commun. *59*, 803 (1994).
30. Semenov A. N.: Sov. Phys. JETP *61*, 733 (1985).
31. Murat M., Grest G. S.: Macromolecules *22*, 4054 (1989).
32. Prochazka K., Limpouchova Z.: Unpublished results.
33. Prochazka K., Kiserow D., Ramireddy C., Tuzar Z., Munk P., Webber S. E.: Macromolecules *25*, 454 (1992).
34. Kiserow D., Prochazka K., Ramireddy C., Tuzar Z., Munk P., Webber S. E.: Macromolecules *25*, 461 (1992).
35. Guilou L., Zinn-Justin J.: Phys. Rev. Lett. 39, 95 (1977); Guilou L., Zinn-Justin J.: Phys. Rev. B *21*, 3976 (1980).
36. Kremer K., Grest G. S.: J. Chem. Phys. *92*, 5057 (1990).

Translated by the author (K. P.).